Experimental and Theoretical Study of the Polarized Infrared Spectra of the Hydrogen Bond in 3-Thiophenic Acid Crystal

ARTICLE *in* JOURNAL OF COMPUTATIONAL CHEMISTRY · JANUARY 2009

Impact Factor: 3.59 · DOI: 10.1002/jcc.21324 · Source: PubMed

5 AUTHORS, INCLUDING:

Najeh Rekik Dr
University of Monastir
2 PUBLICATIONS **12** CITATIONS
SEE PROFILE

Houcine Ghalla
University of Monastir
28 PUBLICATIONS **99** CITATIONS
SEE PROFILE

Henryk T Flakus
University of Silesia in Katowice
96 PUBLICATIONS **1,175** CITATIONS
SEE PROFILE

Magdalena Jabłońska-Czapla
Polish Academy of Sciences
74 PUBLICATIONS **345** CITATIONS
SEE PROFILE

Experimental and Theoretical Study of the Polarized Infrared Spectra of the Hydrogen Bond in 3-Thiophenic Acid Crystal

REKIK NAJEH,[1] GHALLA HOUCINE,[1] HENRYK T. FLAKUS,[2] MAGDALENA JABLONSKA,[2,3] OUJIA BRAHIM[1]
[1]*Laboratoire de Physique Quantique, Faculté des Sciences de Monastir, 5000 route de Kairouan, Tunisia*
[2]*Institute of Chemistry, University of Silesia, 9 Szkolna Street, Pl -40-006 Katowice, Poland*
[3]*Institute of Environmental Engineering of the Polish Academy of Sciences, 34 Maria Curie-Sklodowska Street, 41-819 Zabrze, Poland*

Received 14 February 2009; Revised 11 April 2009; Accepted 14 April 2009
DOI 10.1002/jcc.21324
Published online 4 June 2009 in Wiley InterScience (www.interscience.wiley.com).

Abstract: This article presents the results of experimental and theoretical studies of the ν_{O-H} and ν_{O-D} band shapes in the polarized infrared spectra of 3-thiophenic acid crystals measured at room temperature and at 77 K. The line shapes are studied theoretically within the framework of the anharmonic coupling theory, Davydov coupling, Fermi resonance, direct and indirect damping, as well as the selection rule breaking mechanism for forbidden transitions. The adiabatic approximation allowing to separate the high-frequency motion from the slow one of the H-bond bridge is performed for each separate H-bond bridge of the dimer and a strong nonadiabatic correction is introduced via the resonant exchange between the fast-mode excited states of the two moieties. The spectral density is obtained within the linear response theory by Fourier transform of the damped autocorrelation functions. The approach correctly fits the experimental line shape of the hydrogenated compound and predicts satisfactorily the evolution in the line shapes with temperature and the change in the line shape with isotopic substitution.

 J Comput Chem 31: 463–475, 2010

Key words: H-bond; infrared spectral density; Morse potential; Davydov coupling; quantum direct and indirect damping; Fermi resonances

Introduction

Infrared spectra of hydrogen-bonded systems are considered as a source of information on the dynamics of weak and medium-strength hydrogen bonds. Particular attention of hydrogen bond researchers has been devoted to experimental and theoretical studies.[1–6] Theories have to explain the changes in the infrared spectrum induced by the formation of the H-bond bridge (comparing with free X—H stretching bandshapes), i.e., (i) large increase in the band width, (ii) band asymmetry, (iii) fine structure, (iv) temperature and isotope effects.

Following Hadzi and Bratos[2] and Sandorfy[3] the main features of the line shape are the consequence of large anharmonicity in hydrogen-bonded species, especially between the high frequency mode and the H-bond bridge. These ideas have been incorporated in the quantum formalism to give the strong anharmonic coupling theory. In this framework, for weak hydrogen bonds where it is possible to separate the fast motion of the high frequency mode from the slow one of the H-bond bridge (adiabatic approximation), the oscillator describing the hydrogen bond bridge becomes driven after excitation of the high frequency mode. The driving term increasing linearly with the excitation degree.

The second main theory is dealing with the influence of the medium on the IR ν_{X-H} line shape which may be either direct via its action on the high frequency mode, or indirect via the H-bond Bridge. The direct relaxation, which is corresponding to the first influence, affects simply the lifetime of the first excited state of the high frequency mode whereas the indirect damping takes into account the relaxation of the H-bond bridges via the Louisell and Walker theory of driven damped quantum harmonic oscillator.[7]

Moreover, together with the strong anharmonic coupling between the high and low frequency modes, there is also the possibility of other anharmonicities via Fermi resonances between the first excited state of the fast mode and harmonics or combination bands of some bending modes. It has been shown

Correspondence to: N. Rekik; e-mail: rekik.najeh@fsm.rnu.tn

that these possibilities of Fermi resonances are strongly assisted by the anharmonic coupling between the high and low frequency modes. At last, many H-bonded species involving the same entities in the intermolecular H-bonded complex may form cyclic dimers. Then, in such situations, there is the possibility of resonance between the twined first excited states of the two high frequency modes belonging to each moiety of the dimer. That leads to Davydov coupling which may affect the IR ν_{X-H} line shape.

In a precedent article,[8] we have proposed a general quantum theoretical approach of the ν_{X-H} IR line shape of centrosymmetric cyclic dimers of weakly hydrogen-bonded species. In this model, the adiabatic approximation has been performed for each separate part of the dimer together with a strong nonadiabatic correction via the resonant exchange between the excited states of the two fast mode moieties. The anharmonicity of the slow mode was described by a "Morse" potential[9] whereas the fast mode was considered as harmonic. Both quantum direct (relaxation of the high frequency modes) and indirect (relaxation of the H-bond bridges) dampings of the systems were taken into account.

In this article, we propose a generalization of the previous theoretical approach[8] of ν_{X-H} IR spectra of crystalline centrosymmetric cyclic dimers of hydrogen-bonded species. The difference between the present model and our precedent approach applied to acetylsalicylic acid dimer is the introduction of Fermi resonances by the aid of an anharmonic coupling between the fast mode and one or several bending modes. The bending modes are described by damped quantum harmonic oscillators.

The aim of this article is to apply this model to polarized crystalline 3-thiophenic acid IR spectra. Working within the linear response theory LRT,[10,11] the spectral density (SD) is given by the Fourier transform of the damped autocorrelation functions (ACF) of the dipole moment operator of the fast mode involved in the ν_{X-H} IR transition. The numerical results show that the spectra of 3-thiophenic and its deuterated analog can be successfully reproduced and predict that this simple model dealing with Davydov coupling, Fermi resonances and taking into account quantum direct and indirect damping and anharmonicity of slow mode, is able to reproduce the experimental polarized spectra of the hydrogen and deuterium bond in 3-thiophenic crystals measured at 77 and 298 K by using a minimum number of independent parameters.

It is interesting to note that this model reduces satisfactorily to the approach of Blaise et al.[12] when the slow mode is described by a harmonic potential and Fermi resonances are ignored. Note that this approach was also utilized by Blaise et al.[13] for interpretation of the crystalline spectra of hydrogen-bonded adipic acid crystals but without taking into account the anharmonicity of the H-bond bridge.

Crystal Structure of 3-Thiophenic Acid

Crystals of 3-thiophenic acid (in an abbreviated notation 3TPA) belong to the monoclinic system.[14] The space group is C2/c and $Z = 8$. In a unit cell eight translationally nonequivalent molecules form twisted centrosymmetric cyclic hydrogen-bonded dimers. The unit cell parameters: $a = 13.601$ Å, $b = 5.447$ Å, $c = 15.054 \pm 0.005$ Å, $\beta = 99.10°$. On crystallizing from melt, 3TPA crystals used to develop the "*bc*" face.

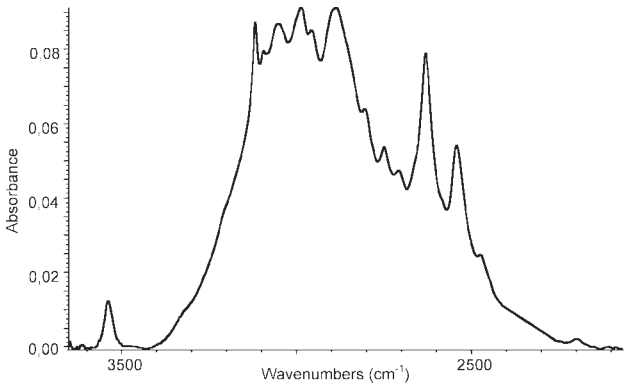

Figure 1. IR spectra of 3-thiophenic acid dissolved in CCl_4, measured in the ν_{O-H} band frequency range.

Experimental

3TPA used for our studies was the commercial substance (Sigma-Aldrich), not subjected to further purification. The d_1 deuterium derivative samples of 3TPA were obtained by evaporation of D_2O solution of the compound at room temperature and under reduced pressure. It was found that the deuterium exchange rate for the COOH groups varied from 50 to 90% for different samples. Crystals of 3TPA, which proved suitable for spectral studies, were obtained by crystallization from melt occurring between two closely spaced CaF_2 windows. In these circumstances 3TPA crystals used to develop the "*bc*" plane. In this way sufficiently thin crystals could be obtained, characterized by their maximum absorbance with the ν_{O-H} band frequency range close to 0.5 at room temperature. From the crystalline mosaic, suitable monocrystalline fragments were selected and then oriented with the help of a polarization microscope. These crystals were exposed to the experiment by use of a metal plate diaphragm with a 1.5-mm diameter hole. Polarized IR spectra were measured by a transmission method. Spectral experiments were performed at room temperature and at the temperature of liquid nitrogen, using polarized IR radiation. In each measurement two different, mutually perpendicular orientations of the electric field vector "**E**" were applied, with respect to the crystalline lattice.

The solid-state spectra were measured with a resolution of 2 cm^{-1}, for the normal incidence of the IR radiation beam, with respect to the developed crystalline face, using a FT-IR Nicolet Magna 560 spectrometer. The polarized spectra of 3TPA single crystals were measured and for two orientations of the electric field vector "**E**." The polarized spectra were measured for the "**E**" vector parallel to the "**c**" axis and also for "**E**" perpendicular to the "**c**" axis, i.e., parallel to the "**b**" axis. Spectra were recorded in a similar way for the deuterium derivative crystals.

Experimental Results

The IR spectra of 3TPA samples measured in the CCl_4 solution are presented in Figure 1. The spectra of the polycrystalline samples of 3TPA, dispersed in KBr pellets, measured at two different temperatures, are shown in Figure 2. To identify the

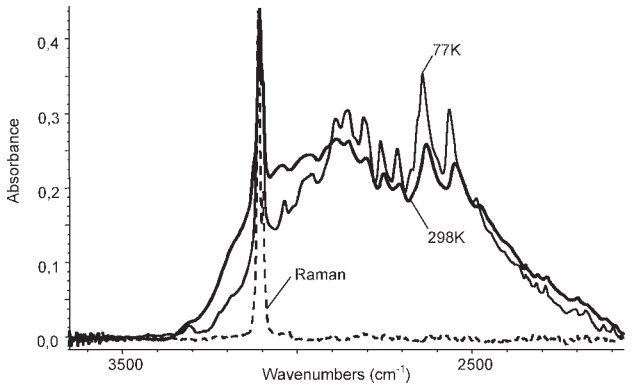

Figure 2. The IR spectra of the polycrystalline samples of 3-thiophenic acid, dispersed in the KBr pellets, measured at two different temperatures. To identify the ν_{C-H} bands and to estimate the impact of these bands on the crystalline ν_{O-H} the Raman spectra of polycrystalline samples of 3-thiophenic acid, measured at room temperature, are also drawn.

V_{C-H} bands and to estimate the impact of these bands on the crystalline V_{O-H}, the Raman spectra of the polycrystalline samples of 3TPA, were measured at the room temperature. The polarized IR spectra of 3TPA single crystals, measured by a transmission method at 298 and 77 K in the V_{O-H} band frequency range, for crystals with the "*bc*" face developed, are presented in Figure 3. Polarized IR spectra of 3TPA single crystals, of a mixed H/D isotopic content (ca. 15% H and 85% D), measured at 298 and at 77 K, in the "residual" ν_{O-H} and the ν_{O-D} band frequency ranges, are presented in Figure 4. Also in this case the spectra were measured for crystals with the developed "*bc*" plane.

Initial Analysis of the Spectra

The polarized spectra of isotopically neat 3TPA crystals (see Fig. 3) consist of two component bands, which are mutually almost proportional in the whole ν_{O-H} band frequency range. This kind of the linear dichroic effect proves that the vibrational exciton coupling mechanism involving the two translationally nonequivalent 3TPA dimers is negligibly weak. This statement finds its further support in the analysis of the dichroic properties

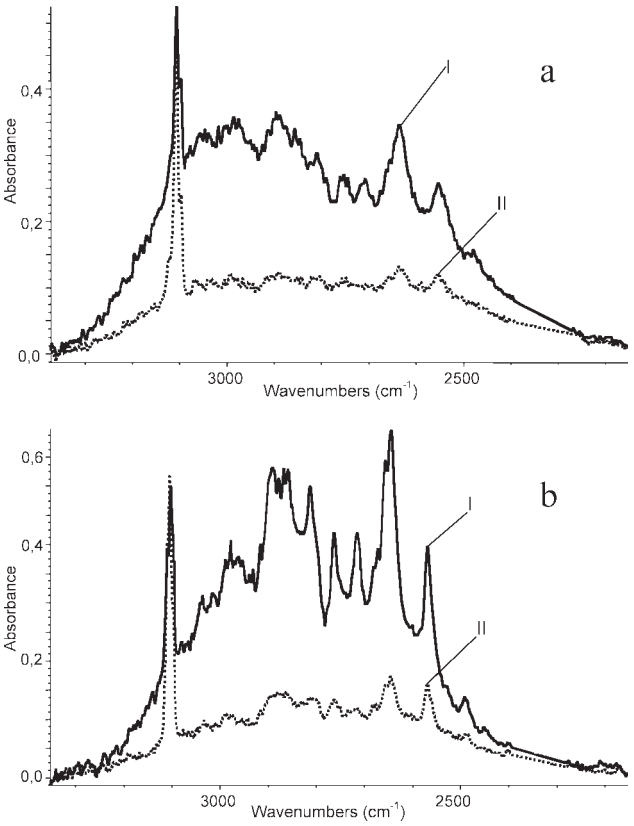

Figure 3. Polarized IR spectra of 3TPA single crystals, measured by a transmission method at 298 and 77 K, in the ν_{O-H} band frequency range. The IR beam of the normal incidence with respect to the "*bc*" crystalline face was applied. In each case, the component spectra were obtained for two orientations of the electric field vector **E**. (I) **E** ∥ c, (II) **E** ⊥ c. (a) Spectra measured at 298 K. (b) Spectra recorded at 77 K.

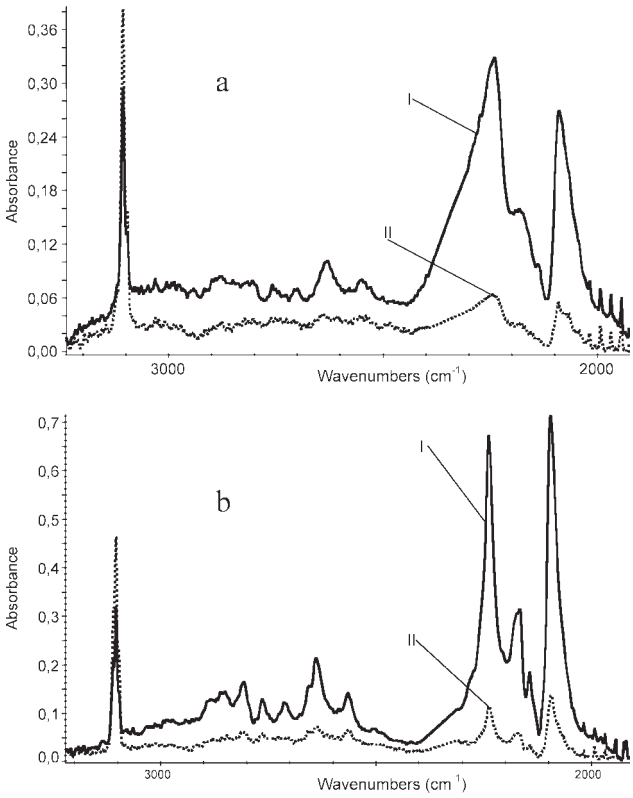

Figure 4. Polarized IR spectra of isotopically diluted (ca. 15% H and 85% D) 3-thiophenic acid single crystals, measured at 298 and 77 K in the "residual" ν_{O-H} and the ν_{O-D} band frequency range. The IR beam of the normal incidence with respect to the "*bc*" crystalline face was applied. In each case, the component spectra were recorded for two orientations of the "**E**" vector. (I) **E** ∥ c, (II) **E** ⊥ c. (a) 298 K. (b) 77 K.

of the "residual" ν_{O-H} band, which is the attribute of the protons, nonreplaced by deuterons in isotopically diluted 3TPA samples. Replacement of the major part of the protons by deuterons practically did not change the polarized component band contour shapes as well as the proportionality relation between them (see Fig. 4).

The reported invariability of the ν_{O-H} band contour shape accompanying to the increasing *H*/*D* isotopic dilution rate is the manifestation of dynamical cooperative interactions involving hydrogen bonds, acting in crystal lattices composed with cyclic hydrogen bond dimers. As the consequence, the distribution of protons and deuterons in hydrogen bond lattices of isotopically diluted crystals is very often nonrandom. The same mechanism is most probably responsible for the spectral properties of 3TPA crystals. Isotopic dilution leads to a nonrandom distribution of protons and deuterons in the hydrogen bond lattices of 3TPA crystals. It was found recently that only the symmetric hydrogen bond dimers of the *HH*- or *DD*-type, i.e. containing two protons or two deuterons in their hydrogen bridges, determine the spectral properties of the crystals. Concentration of the *HD*-type dimers, of the mixed H/D content is negligibly small. Therefore, the 3TPA crystal spectra remain invariant in the widest range of *H*/*D* concentration rates. This so-called *H*/*D* isotopic "self-organization" effect[15,16] observed in the IR spectra of diverse hydrogen bond dimeric systems, e.g., existing in benzoic acid crystals.[17]

All these facts justify accepting the assumption, that 3TPA cyclic, centrosymmetric dimers, containing two identical hydrogen isotope atoms in their hydrogen bridges, are the structural units of the lattice responsible for generation of the main crystal spectral properties of the hydrogen bond in 3TPA crystals. The interdimer vibrational Davydov-couplings involving the translationally nonequivalent 3TPA dimers from each unit cell of the lattice are negligibly weak and they practically do not affect the crystalline spectra. On the other hand, the crystalline spectra are fairly similar to the corresponding spectrum of 3TPA recorded for CCl_4 solution (compare the spectra from Figs. 3 and 4). This proves that even in the isotopic dilution centrosymmetric dimers, each with identical hydrogen isotope atoms in its hydrogen bridges, are the bearers of the crystal main spectral properties in the ν_{O-H} and ν_{O-D} band frequency range.

Theory

This approach is working within the linear response theory according to which the spectral density (SD) is the Fourier transform of the autocorrelation function (ACF) at temperature T of the dipole moment operator involved in the ν_{X-H} IR transition.

Let us consider a cyclic dimer of carboxylic acid with two H-bond bridges. The two parts of the dimer are labeled $r = 1, 2$. For cyclic symmetric dimers of H bonds, there are two degenerate high frequency modes and two degenerate low frequency H-bond vibrations, as shown in Figure 5a. The adiabatic approximation leads to description of each moiety by effective Hamiltonians of the H-bond bridge: for a single H-bond bridge, this effective Hamiltonian is either that of an harmonic oscillator if the fast mode is in its ground state, or that of a driven harmonic

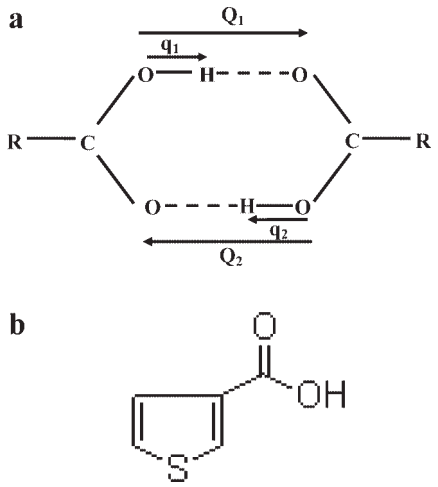

Figure 5. (a) A cyclic centrosymmetric H-bonded dimer (carboxylic acid). (b) The monomers of 3-thiophenic acid.

oscillator if the fast mode is excited. When one of the two identical fast modes is excited, then, because of the symmetry of the cyclic dimer, and of coupling V° between the two degenerate fast mode excited states, an interaction occurs (Davydov coupling) leading to an exchange between the two identical excited parts of the dimer. Of course, this interaction between degenerate excited states is of nonadiabatic nature although the adiabatic approximation has been performed in order to separate the high and low frequency motions. Besides, because of the symmetry of the dimer, there is a symmetry C_2 parity operator which exchanges the two moieties of the system. This operator exchanges the coordinates Q_i of the two H-bond bridges of the cyclic dimer according to:

$$C_2Q_1 = Q_2 \quad \text{and} \quad C_2Q_2 = Q_1 \tag{1}$$

After symmetrization, the centrosymmetric cyclic dimer split into symmetric (g) and antisymmetric (u) parts. The basic physical parameters dealing with this system are as follows: ω° (Ω), the vibration angular frequency of the two degenerates fast modes moieties; α°, the dimensionless strong anharmonic coupling parameter; Ω, vibration angular frequency of the two degenerates H-bond bridge moieties; β_e, the dimensionless parameter characterizing the Morse potential width; D_e, the dissociation energy of the H-bond bridge; γ° (γ), the direct (indirect) damping parameter of the fast (slow) mode; V°, the Davydov coupling parameter; γ_i^δ, the damping parameter of the bending mode; ω^δ, the angular frequency of the bending mode; f_i, Fermi coupling parameter; Δ_i^0, the angular frequency gap between the fast the bending modes; T, absolute temperature.

The Basic Equations

The infrared spectral density $I_{Dav}(\omega)$ of an hydrogen bond in the dimer may be related, within the linear response theory, to the autocorrelation function $G_{Dav}(t)$ of the transition dipole

momentum of the fast mode $X-\vec{H}...Y$, through the following Fourier transform:

$$I_{\mathrm{Dav}}(\omega) \propto 2\mathrm{Re}\int_0^\infty G_{\mathrm{Dav}}(t)\exp(-i\omega t)dt \tag{2}$$

In the presence of direct damping, the quantum autocorrelation function $G_{\mathrm{Dav}}(t)$ may be written,[18]

$$G_{\mathrm{Dav}}(t) = \mathbf{G}^{\circ}(t)\exp(-\gamma^{\circ}t) \tag{3}$$

where γ° is the direct damping parameter of the fast mode. $\mathbf{G}^{\circ}(t)$ is the autocorrelation function without damping. It may be written, in a general way:

$$\mathbf{G}^{\circ}_{\mathrm{Dav}}(t) \propto tr\left[\exp\{-\mathbf{H}_{\mathrm{Tot}}/kT\}\mathbf{q}\,\exp\left\{i\frac{\mathbf{H}_{\mathrm{Tot}}t}{\hbar}\right\}\mathbf{q}\,\exp\left\{-i\frac{\mathbf{H}_{\mathrm{Tot}}t}{\hbar}\right\}\right] \tag{4}$$

That, in order to obtain the spectral density [eq. (2)], we need to construct and diagonalize the full Hamiltonian $\mathbf{H}_{\mathrm{Tot}}$.

Within the strong anharmonic coupling theory and the anharmonic approximation for the H-bond bridge which is described by a Morse potential, the corresponding Hamiltonians of the slow and high frequency modes of the two moieties of the dimer are, respectively, given, using dimensionless operators, by the following expressions:

$$\left[\hat{H}_{\mathrm{Slow}}\right]_i = \frac{1}{2}\hat{P}_i^2\hbar\Omega + D_e\left[1-\exp\left(-\beta_e\hat{Q}_i\sqrt{\frac{M\Omega}{\hbar}}\right)\right]^2 \quad \text{where } i=1,2 \tag{5}$$

$$\left[\hat{H}_{\mathrm{Fast}}\right]_i = \frac{1}{2}(\hat{p}_i^2+\hat{q}_i^2)\hbar\omega(\hat{Q}_i) \tag{6}$$

In these equations, $\hat{P}_i$ are the dimensionless conjugate momenta of the H-bond bridges dimensionless coordinates $\hat{Q}_i$ of the two moieties, whereas $\hat{p}_i$ and $\hat{q}_i$ are the dimensionless coordinates and the conjugate momenta of the two degenerate high frequency modes of the two moieties. Ω and M are the angular frequency and the reduced mass of the H-bond bridge, whereas $\omega(\hat{Q}_i)$ is that of the high frequency mode which is supposed to depend on the coordinate of the H bond bridge. D_e is the dissociation energy of the H-bond bridge and β_e is given by:

$$\beta_e = \Omega\sqrt{\frac{M}{2D_e}}\sqrt{\frac{\hbar}{M\Omega}} \tag{7}$$

Using a Taylor development of the Morse potential[9] given by:

$$\hat{V}_{\mathrm{Morse}}(Q) = D_e\left[1-\exp\left(-\beta_e\hat{Q}\sqrt{\frac{M\Omega}{\hbar}}\right)\right]^2$$

Equation (5) can be rewritten as the sum of the hamiltonian of a quantum harmonic oscillator and an anharmonic potential $V^{\circ\circ}$:

$$\left[\hat{H}_{\mathrm{Slow}}\right]_i = \left[\hat{H}^0_{\mathrm{Slow}}\right]_i + \hat{V}^{\circ\circ} \tag{8}$$

where $\left[\hat{H}^0_{\mathrm{Slow}}\right]_i$ and $\hat{V}^{\circ\circ}$ are respectively given by:

$$\left[\hat{H}^0_{\mathrm{Slow}}\right]_i = \frac{1}{2}(\hat{P}_i^2+\hat{Q}_i^2)\hbar\Omega \tag{9}$$

$$\hat{V}^{\circ\circ}(\hat{Q}_i) = D_e\sum_{n=3}^{\infty}\frac{(-1)^n(2^n-2)}{n!}\left(\beta_e\hat{Q}_i\sqrt{\frac{M\Omega}{\hbar}}\right)^n \tag{10}$$

Following Maréchal and Witkowski,[19] expansion to first-order of the angular frequency of the fast mode with respect to the coordinate of the H-bond bridge leads to write:

$$\omega(\hat{Q}_i) = \omega^{\circ} + \alpha^{\circ}\Omega\hat{Q}_i \tag{11}$$

Here, ω° is the angular frequency of the two degenerate fast modes when the corresponding H-bond bridge coordinates are at equilibrium, whereas α° is a dimensionless parameter which will appear to be an anharmonic coupling parameter.

In the presence of damping, the thermal bath may be figured, by an infinite set of harmonic oscillators, and its coupling with the H-bond bridge are described by terms which are linear in the position coordinates of the bridge and of the bath oscillators:

$$H_{\mathrm{Damp}} = \sum\frac{1}{2}[\tilde{p}_r^2+\tilde{q}_r^2]\hbar\omega_r + \sum\tilde{p}_r[\hat{Q}_1+\hat{Q}_2]\hbar g_r \tag{12}$$

Here, $\tilde{q}_r$ are the dimensionless position coordinate operators of the oscillators of the bath. $\tilde{p}_r$ are the corresponding conjugate momenta, obeying the usual quantum commutation rules, ω_r are the corresponding angular frequencies and g_r are the coupling between the H-bond bridges and the oscillators of the bath. Within the adiabatic approximation, the hamiltonian of each moiety of the dimer take the form of sum of effective hamiltonians which are depending on the degree of excitation of the fast mode according to:

$$[\hat{H}_{\mathrm{Adiab}}]_i = \sum[\hat{H}^{\mathrm{o}\{k\}}]_i|\{k\}_i\rangle\langle\{k\}_i| \qquad i=1,2\ ;\ k=0,1 \tag{13}$$

$$[\hat{H}^{\mathrm{o}\{k\}}]_i = \frac{1}{2}\hat{P}_i^2\hbar\Omega + D_e\left[1-\exp\left(-\beta_e\hat{Q}_i\sqrt{\frac{M\Omega}{\hbar}}\right)\right]^2 + k\alpha^{\circ}\hat{Q}_i\hbar\Omega + k\hbar\omega^{\circ} \tag{14}$$

We have also used a second approach for the introduction of the Morse potential. In this context, the matrix elements of $\mathbf{V}_{\mathrm{Morse}}(\mathbf{Q})$ in the basis where $\mathbf{H}_{\mathrm{Adiab}}$ is diagonal are of the form:

$$\langle(m)|\langle\{j\}|\hat{V}^{\circ\circ}(\hat{\mathbf{Q}})|\{k\}\rangle|(n)\rangle = \langle\{m\}|\hat{V}^{\circ\circ}(\hat{\mathbf{Q}})|\{n\}\rangle\delta_{j,k} \tag{15}$$

The right hand side matrix elements of this last equation are calculated in our precedent article.[20] As a consequence the matrix elements are:

$$\langle n|\hat{V}^{\circ\circ}(\hat{\mathbf{Q}})|m\rangle = D_e\{\delta_{n,m} - 2V(n,m,\beta) + V(n,m,2\beta)\} \quad (16)$$

where

$$V(n,m,a) = \sqrt{n!m!}\sum_{p=0}^{\min(n,m)}(-\frac{a}{\sqrt{2}})^{n+m-2p}\frac{1}{p!(n-p)!(m-p)!} \quad (17)$$

In our calculations, the dimension of the basis involved in the eigenvalue equations (15) and (13) are increased progressively until the theoretical IR line shape obtained become stabilized. Note that these two approaches for the introduction of Morse potential [eqs. (9) and (15)] lead to same results.

An excitation, of the fast mode of one moiety of the dimer is resonant with the excitation of the other moiety. Thus, a strong nonadiabatic correction[19] i.e., a Davydov coupling V_{12}, occurs between the two resonant states after excitation of one of the two fast modes, so that the full Hamiltonian of the two moieties, is given by the equations:

$$\text{with} \qquad \hat{H}_{\text{Tot}} = \left[\hat{H}_{\text{Adiab}}\right]_1 + \left[\hat{H}_{\text{Adiab}}\right]_2 + \hat{V}_{12} + \hat{H}_{\text{Damp}} \quad (18)$$

$$\hat{V}_{12} = \hbar V^{\circ}[|\{1\}_1\rangle\langle\{0\}_2| + |\{0\}_1\rangle\langle\{1\}_2|] \quad (19)$$

where V° is the Davydov coupling parameter.

On the other hand, because of the centrosymmetric of the cyclic dimer, the ACF may be split into symmetric parts (g) and antisymmetric parts (u). It can be written following:

$$G_{\text{Dav}}(t) = [G(t)]_g[[G^+(t)]_u + [G^-(t)]_u] \quad (20)$$

In this equation, $[G(t)]_g$ is the g ACF of the dipole moment operator of the fast mode which is affected by the strong anharmonic coupling and the indirect damping of the H-bond bridge.

It has been found[21,22] using important results of Louisell and Walker[7] that the reduced ACF $[G(t)]_g$ can be written,[13] after taking into account the natural line width of the excited state of the fast mode, in the following closed form:

$$[G(t)]_g \propto e^{i\omega^{\circ}t}e^{-i\frac{\alpha^{\circ}}{2}\Omega t}e^{-i[\frac{\beta}{\sqrt{2}}]^2\Omega t}e^{-i[\frac{\beta}{\sqrt{2}}]^2[\langle n\rangle+\frac{1}{2}]} (2e^{\frac{-\gamma t}{2}}\cos\Omega t - e^{-\gamma t})e^{i|\beta|^2e^{\frac{-\gamma t}{2}}}\sin\Omega t \quad (21)$$

In this equation, $\langle n\rangle$ and β are respectively the thermal average of the occupation number and the effective dimensionless anharmonic coupling parameter related to α°. These terms are given by:

$$\beta = \alpha^{\circ}\frac{[4\Omega^4 + \gamma^2\Omega^2]^{1/2}}{\sqrt{2}(\Omega^2 + \frac{\gamma^2}{4})} \quad (22)$$

$$\langle n\rangle = \frac{1}{e^{\frac{\hbar\Omega}{kT}} - 1} \quad (23)$$

On the other hand, $[G^+(t)]_u$ and $[G^-(t)]_u$ are the two u ACFs dealing with the corresponding u part, which are affected only by the Davydov coupling and by the anharmonicity of the H-bond Bridge. They are given by[23]:

$$[G^{\pm}(t)]_u \propto \sum_n\sum_{\mu} e^{-\frac{n\hbar\Omega}{kt}}[1 \pm (-1)^{n\mu+1} + \eta[1 - (-1)^{n\mu+1}]^2]^2 \times |C^{\pm}_{n\mu,\mu}|^2 e^{i\omega^{\pm}_{\mu}t}e^{-in_{\mu}\Omega t} \quad (24)$$

where the parameter η is a dimensionless parameter reflecting the fact that in the real cyclic dimers, it is not possible to split rigorously the equations of the system into a (g) and (u) parts. This parameter looks like some breaking of the IR selection rule forbidding the A_g transition in cyclic dimer of carboxylic acids.

Besides, $C^{\pm}_{n\,\mu,\mu}$ are the expansion coefficients of the eigenvectors on the basis of the eigenstates $|n\rangle$ of the Hamiltonian of the quantum harmonic oscillator.

$$\psi^{\pm}_{\mu} = \sum C^{\pm}_{n_{\mu},\mu}|n\rangle \quad (25)$$

In this equation, $C^{\pm}_{n_{\mu},\mu}$ are the eigenvalues of the time-independent Schrödinger equations involving Hamiltonians of driven undamped quantum harmonic oscillators describing both the fast and slow modes of the two moieties of the dimer perturbed by the Davydov coupling and the anharmonic part $V^{\circ\circ}$ of the Morse potential.

Following the eqs. (2), (20), and (24), the spectral density (SD) of the dimer involving Davydov effect is the Fourier transform of this ACF, i.e.,

$$I(\omega) \propto 2\text{Re}\int_0^{\infty}[G(t)]_g[[G^+(t)]_u + [G^-(t)]_u]\exp(-\gamma^{\circ}t)\exp(-i\omega t)dt \quad (26)$$

That may be written formally:

$$I(\omega) \propto I^+(\omega) + I^-(\omega) \quad (27)$$

$$\text{with respectively } I^{\pm}(\omega) \propto \sum_m\sum_n\{P_{m,n}\}\sum_{n_{\mu}}\sum_n\{A^{n_{\mu},\mu}_{m,n}\} \quad (28)$$

In view of the above equations, the components appearing here are given by the following equations[12,24]:

$$\{A^{n_{\mu},\mu}_{m,n}\} = e^{\lambda\bar{n}_{\mu}}\left[1 \pm (-1)^{n_{\mu}+1}\right]^2 \times |C^{\pm}_{n_{\mu},\mu}|^2\{I^{\pm}_{mnn_{\mu},\mu}(\omega)\}$$

$$\{I^{\pm}_{mnn_{\mu},\mu}(\omega)\} \propto \frac{\gamma_{m,n}}{(\omega - \Omega^{\pm}_{mnn_{\mu},\mu})^2 + (\gamma_{m,n})^2}, \quad (29)$$

$$\Omega^{\pm}_{mnn_{\mu},\mu} = \omega^{\circ} - [(m - n + n_u)\Omega - \omega^{\pm}_{\mu}] - \alpha^{\circ}\sqrt{2\Omega}, \quad (30)$$

$$\gamma_{m,n} = (m+n)\gamma + \gamma^{\circ}, \tag{31}$$

$$P_{m,n} = \frac{[1+\langle n\rangle]^m \langle n\rangle^n |\frac{\beta}{\sqrt{2}}|^{2(m+n)}}{m!n!} \tag{32}$$

Recall that, despite its generality, the present model is involving two important approximations. The first important one that it is not possible to split rigorously the equations of the system into a g and u parts, the second approximation is the adiabatic approximation for the two separate moieties before taking into account Davydov coupling. Besides these approximations, one may quote other ones which are probably of smaller importance:

i. neglect of the modulation of the equilibrium positions of the fast modes and the quadratic dependence of their frequencies on (Q_i) as confirmed by several experimental correlations,
ii. independence of the Davydov coupling with respect to Q_i,
iii. neglect of electrical anharmonicity, and
iv. neglect of the anharmonicities of the fast mode (tunneling through the potential barrier).

Combined Davydov Coupling and Fermi Resonances

Now suppose the situation where we take into account the Fermi resonance effect. This later is resulting from the interactions occurring between the first excited state of the high frequency mode and the first harmonic of some bending modes. As it was stated by Maréchal and Witkowski,[19] the dynamics of the stretching vibrations of an isolated hydrogen bond X—H...Y may be mostly understood as the result of a strong anharmonic coupling between the fast X—H and the slow X—H...Y stretching modes. From a full quantum mechanical point of view, the treatment of this anharmonic coupling may be performed within the adiabatic approximation. Besides, for a single H-bond open dimer, the Fermi resonance is the result of an anharmonic coupling between the fast and bending modes. All these vibrating modes will be separately considered as quantum harmonic oscillators, as it is generally performed, whose angular frequencies are ω° (fast stretching modes), $\omega^{\circ\circ}$ (slow stretching modes), and ω^{δ} (bending modes).

The Davydov coupling will occur through a resonant exchange between the excited states of the two fast modes. If Fermi resonances are taken into account, one has to consider one fast mode, one slow mode and one bending mode for each hydrogen bond of the cyclic dimer according to Figure 1b**.** As a consequence, one may define $|\{k\}_i\rangle$ and $|(m)_i\rangle$ the kth and mth eigenstates of respectively the fast and slow modes of the ith H-bond, and $|[u]_i\rangle$ the uth eigenstate of the bending mode which is coupled to the fast mode of the ith H-bond. Using these definitions, the model of cyclic dimers involving Fermi resonances, Davydov coupling, and direct damping of the fast and bending modes requires the following interactions involving the six basis modes.

It was shown[24] that the Fermi resonances affect only the g state of the system. As a consequence, the u G_g (t) autocorrelation functions are not modified.

In the presence of Davydov coupling and Fermi resonances, the ACF can be written following:

$$[G(t)]_g \propto \sum_n \sum_\mu e^{-\lambda m} |a_{\{\mu,0,m\}_g}|^2 [e^{i\{\omega_\mu\}_g t/\hbar}] e^{-im\Omega t} \tag{33}$$

where $\{\omega_\mu\}_g$ are the eigenvalues appearing in eq. (34) whereas, $\alpha_{\{\mu,\ 0,\ m\}g}$ are the expansion coefficients defined by eq. (35).

$$[H_D^F]_g |\phi_\mu\rangle_g = \hbar |\phi_\mu\rangle_g \{\omega_\mu\}_g \tag{34}$$

$$|\phi_\mu\rangle_g = \sum_l \sum_m \{a_{\mu,l,m}\}_g |\Phi_{l,m}\rangle_g \tag{35}$$

The g states involved in the above expansions are defined by:

$$|\{\Psi_{0,m}\}_g\rangle = |\{1\}_g\rangle |\{0_1\}_g\rangle |[0_2]_g\rangle |(m)_g\rangle \tag{36}$$

$$|\{\Psi_{1,m}\}_g\rangle = |\{0\}_g\rangle |\{2_1\}_g\rangle |[0_2]_g\rangle |(m)_g\rangle \tag{37}$$

$$|\{\Psi_{2,m}\}_g\rangle = |\{0\}_g\rangle |\{0_1\}_g\rangle |[2_2]_g\rangle |(m)_g\rangle \tag{38}$$

Here, the kets $|\{k\}_g\rangle$, $|(m)_g\rangle$, and $|[l]_g\rangle$ are the g eigenstates of respectively the symmetrized high frequency quantum harmonic oscillator, the slow frequency quantum harmonic oscillator, and the bending frequency quantum harmonic oscillator. The Fermi resonance mechanism, characterized by the coupling parameter f_i, is described by the following coupling operators $\hbar f$ which express the nonresonant exchanges between the state $|\{1\}_j\rangle$ of the jth fast mode and second damped excited state $|\{2\}_j\rangle$ of the jth bending mode. The introduction of the Fermi resonance coupling effects in the line shape is presented by the complexes angular frequency gap Δ_i:

$$\Delta_i = \Delta_i^{\circ} - i\gamma_i^{\delta} \tag{39}$$

$$\Delta_i^{\circ} = -\omega^{\circ} - 2\omega_i^{\delta} \tag{40}$$

where ω_i^{δ} is the frequency of the bending modes. The imaginary part in this gap is related to the lifetime of the corresponding excited states.

Some Trends Appearing in Special Situations

Before looking at the features displayed by the general spectral density eq. (26), it may be of interest to focus on the link between this spectral density and those previously obtained in the literature. The present model reduces to other already well-

Table 1. Parameters Used for Fitting Experimental H-3-Thiophenic Acid Spectra.

H-species Pol (°)	T (K)	Ω (cm^{-1})	ω° (cm^{-1})	α°	V° (Ω)	γ° (Ω)	γ (Ω)	η
0	77	80	3070	1.5	−1.0	0.25	0.01	0.75
90	77	75	2990	1.5	−0.855	0.18	0.1	0.65
0	298	75	3005	1.35	−1.27	0.17	0.1	0.95
90	298	80	3000	1.5	−1.68	0.3	0.1	0.95

known models when some "ingredients" are neglected. In the absence of anharminicity of the slow mode (Morse potential), it directly reduces to that of Blaise et al.[13] Additionally neglecting the Fermi resonances make this model to reduce to that of Blaise et al.[12] This model, which is very general, also reduces satisfactorily to: (i) the approach of Maréchal and Witkowski,[19] which ignores the damping, (ii) that of Rosch and Ratner[18] which takes only into account the "direct" damping, (iii) that of Boulil et al.,[25,26] which considers only the indirect damping. Recall that this last quantum model reduces in the classical limit to that of Blaise et al.,[27] which reduces in turn, after some approximations, to the semiclassical model of Robertson and Yarwood.[28,29] Besides, this last semiclassical model reduces to that of Bratos[30]; For a more general model involving Fermi resonances, see ref. 31, in the slow modulation limit. Finally, in the absence of Fermi resonances and of quantum indirect damping, the present model reduces to that of Flakus[32] and in the special situation of one Fermi resonance and in the absence of quantum direct and indirect dampings, it is equivalent to the model of Wojcik[33] dealing with crystalline H-bonded species in which the interaction of the two dimers of the unit cell is ignored.

The υ_{O-H} and υ_{O-D} Band Shapes in Crystalline 3-Thiophenic Acids

The present model is applied to polarized 3-thiophenic acid (see Fig. 5b: monomer 3-thiophenic formula) and to its deuterated in crystalline phase. The spectral densities are computed by eq. (26) after construct and diagonalize the total Hamiltonian H_{Tot} in a truncated basis. The stability of the computed spectra with respect to the size of this basis set was carefully checked. The stability of the spectra was also checked versus the order of the Taylor expansion of the Morse potential: full numerical stability was achieved for the order 65.[34] We used this value in our calculations.

To prove the validity of this approach, it is of interest to comment the importance of the parameters used to fit the experimental line shapes. We have selected for the dissociation energy of the H-bond bridge, the value $D_e = 2100\ cm^{-1}$, then $\beta_e = 0.189$.[35] The υ_{X-H} of the fast mode of the 3-thiophenic acid used in the calculation is around $3000\ cm^{-1}$. Note that, according to Maréchal and Witkowski theory,[19] the angular frequency ω° of the high frequency mode must be decreased on D isotopic substitution of the proton involved in the H-bonds. More precisely, in the D isotopic substitution of the protons of the hydrogen bond bridge in the dimer, the both angular frequency of the fast mode and the anharmonic coupling parameter must be reduced by the factor $\frac{1}{\sqrt{2}}$, whereas the frequency Ω of the H-bond bridge has no reason to be modified. The sets of parameters used to fit the experimental line shapes are reported in Tables 1 and 2.

Following Witkowski and Wójcik,[36] if we are interested in the D isotopic substitution of the protons of the H-bond bridge in the dimer at a given temperature T, one may reasonably assume, in harmonic approximation for the H-bond Bridge, that the angular frequency ω° of the high frequency mode and the anharmonic coupling parameter α° are decreased by $\sqrt{2}$. In harmonic approximation, we have[36]:

$$\left(\frac{\omega^\circ H}{\omega^\circ D}\right) = \left(\frac{\alpha^\circ H}{\alpha^\circ D}\right) = \sqrt{2} \tag{41}$$

To improve the validity of the present model, let us comment the magnitude of the parameters that we have used. Both the anharmonic coupling parameter and the angular frequencies of the high frequency mode for the 3TPA-D, in all treated situations (T = 77 and 298 K and for different polarizations), their magnitudes are decreased by factors which are different from $\sqrt{2}$. This result is in agreement with theory when passing from the H to the D species and when the slow mode is assumed to be of "Morse" type (anharmonic potential). Note that in the work of Blaise et al.,[12] both the anharmonic coupling parameter and the angular frequencies of the high frequency mode are decreased by a factor very near $\sqrt{2}$. However in our treatment, for 3TPA, this reduction by the factor $\sqrt{2}$ leads, respectively, for the angular frequencies of the D isomer at 77 K and $P = 0^\circ$, 2170 cm^{-1} in place of 2147 cm^{-1} and 2114 cm^{-1} in place of 2169 cm^{-1} for the case when the polarization is $P = 90^\circ$ at the same temperature 77 K. The same observation was elucidated for the temperature 298 K. Indeed, the reduction by the factor $\sqrt{2}$ leads to the following values: 2124 in place of 2154 at $P = 0^\circ$ and 2121 in place of 2164 when the polarization is $P = 90^\circ$. For the corresponding anharmonic coupling parameters the same reduction leads, in the case when T = 77 and $P = 0^\circ$ to 1.06 in place of 0.265 and to 0.954 in place of 0.341 at T = 300 K for the same polarization. As we can see from the inspection of tables, the anharmonic coupling parameters ratios $r_\alpha = r_\alpha = (\frac{\alpha^\circ H}{\alpha^\circ D})$ and the angular frequency ratios $r_\omega = (\frac{\omega^\circ H}{\omega^\circ D})$ between the fast and slow modes of two separate H-bond, in our calcula-

Table 2. Parameters Used for Fitting Experimental D-3-Thiophenic Acid Spectra.

D-species Pol (°)	T (K)	Ω (cm^{-1})	ω° (cm^{-1})	α°	V° (Ω)	γ° (Ω)	γ (Ω)	η
0	77	90	2147	0.265	−0.571	0.16	0.1	0.95
90	77	75	2169	0.366	−0.843	0.28	0.1	0.95
0	298	75	2154	0.341	−0.907	0.15	0.1	0.95
90	298	85	2164	0.341	−0.83	0.1	0.1	0.85

tions of the $\upsilon_{SO-H(D)}$ bands are very different to $\sqrt{2}$. We have used:

$$\left(\frac{\alpha^\circ H}{\alpha^\circ D}\right)_{T=77\text{ K},P=0^\circ} = 5.66 \quad \left(\frac{\alpha^\circ H}{\alpha^\circ D}\right)_{T=298\text{ K},P=0^\circ} = 3.95$$
$$\left(\frac{\alpha^\circ H}{\alpha^\circ D}\right)_{T=77\text{ K},P=90^\circ} = 4.09 \quad \left(\frac{\alpha^\circ H}{\alpha^\circ D}\right)_{T=298\text{ K},P=0^\circ} = 4.39 \tag{42}$$

$$\left(\frac{\omega^\circ H}{\omega^\circ D}\right)_{T=77\text{ K},P=0^\circ} = 1.43 \quad \left(\frac{\omega^\circ H}{\omega^\circ D}\right)_{T=298\text{ K},P=0^\circ} = 1.395$$
$$\left(\frac{\omega^\circ H}{\omega^\circ D}\right)_{T=77\text{ K},P=90^\circ} = 1.378 \quad \left(\frac{\omega^\circ H}{\omega^\circ D}\right)_{T=298\text{ K},P=90^\circ} = 1.386 \tag{43}$$

These numerical results related to ratios $\left(\frac{\alpha^\circ H}{\alpha^\circ D}\right)$ for different temperatures and polarizations show an anomalous isotopic effects which may be connected with the neglect of mechanical anharmonicity of the X—H stretching motions. The values obtained here are in satisfactory agreement with the experimental data reported by Odinokov and Iogansen[37] for complexes of carboxylic acids with various bases. Besides, these values are comparable to those found in our recent work dealing with the *H*/*D* isotopic effects in H-bond spectra.[38] However, these ratios are different from those used by Blaise et al.,[12] and by Boczar et al.,[39] since in their approaches, low and high-frequency hydrogen stretching vibrations in individual hydrogen bonds are assumed to be harmonic whereas in the present work we use a Morse potential in order to describe the anharmonicity of the H-bond bridge. Recall that the removal of the harmonic approximation for the slow modes by introducing Morse potential in place of harmonic one has been done by Leviel and Maréchal[40] in a model similar to the present one, involving cyclic dimer, however without damping. They have shown that the value of the angular frequency of the slow mode which must be used to fit the experimental line shape is more close to the experimental value when the anharmonicity of the bridge is introduced. Morse potential for the low frequency mode has been also used by Wojcik[41] in theoretical interpretation of IR spectra of the gaseous $(CH3)_2$ O. . .H (D) Cl complex.

The numerical simulation shows that this model reproduces satisfactorily the main features of the experimental IR line shapes the of crystalline 3-thiophenic-H and 3-thiophenic-D dimers for two different temperatures 77 and 298 K, especially for the high and low frequencies tails, but less satisfactorily the details of the fine structure. Figure 2 is dealing with the comparison of theoretical and experimental line shapes, for hydrogenated (υ_{O-H}) and deuterated (υ_{D-H}) crystalline 3-thiophenic acid, for 0° and 90° polarizations, at 77 and 298 K, when it is assumed that Fermi resonances are missing.

Consider now the general physical situation in which Fermi resonances are occurring and for which the spectral density is given by eqs. (20), (26), and (33). The procedure we have used is the fitting of the experimental line shapes by optimizing the values of the basic parameters. We have performed numerical experimentation by increasing progressively the number of Fermi resonances. We have observed that the quality of the fitting increases progressively but more and more slowly with this number. We have observed that a good compromise between this number and the accuracy of the fitting may be the use of three Fermi resonances.

Comparison of Figures 6 and 7 show that the incorporation of Fermi resonances does not improve sensitively the accuracy of the theoretical fitting. Besides, comparison of the values of the basic parameters used for the fitting and appearing in Tables 1 and 2, i.e., the value of the angular frequencies ω° and Ω of the fast and slow modes, and those of the anharmonic coupling parameter α and of the Davydov coupling V°, which have no reason to be modified by the polarization or the temperature, shows that for both the O—H species and the O—D species, the stability of the basic parameters with respect to the polarization and the temperature, is not improved by the incorporation of Fermi resonances. That leads to conclude that Fermi resonances seem to do not play a significant role in the IR spectra of the 3-thiophenic acid dimer.

Figure 7 reports the comparisons between the experimental line shapes measured by Flakus and the corresponding theoretical ones calculated in this way by the aid of eqs. (20), (26), and (33). In this figure, the line shapes are reproduced, respectively, at 77 and 298 K. The values of the parameters used for the calculations are reported in Tables 1–4. Note that in our computation, we have assumed, as previously,[23,24] and following Flakus,[42] that the η parameter involved in eq. (24) cannot be zero at very low temperatures and decrease when temperature is rising especially for the H-bonded species.

Now, let us look at the comparisons between theoretical and experimental line shapes given by Figures 6 and 7**.** To obtain a good agreement with the experimental line shapes, we have take into account some breaking of the IR selection rule for the centrosymmetric cyclic dimer, via a large amount ($\eta = 0.65. . .0.95$) of forbidden A_g transition. Recall that in general way the quality of the fitting is weakly improved by taking small values for η which lying between 0 and 1. This assumption was initially introduced by Flakus.[42] This is a general trend which has been observed recently in the cases of the centrosymmetric cyclic dimers of gaseous acetic acid.[12] Note that, according to Flakus hypothesis, the lack of "forbidden" transition ought to be stronger in the solid state than in the gaseous one and we must keep in mind that the Flakus assumption has been seen by this author to be unavoidable in diverse crystalline H-bonded carboxylic acids such as for instance glutaric,[43] pimelic,[44] benzoic,[45] phenyl acetic 1-and -2 naphtyl,[46] and cinnamic[47] acids and particularly in centrosymmetric H-bonded dimers such as 2-hydroxybenzothiazole and 2-mercaptobenzothiazole.[48] The problem of the "selection rule breaking" in the spectra is, in our opinion, a real problem. Flakus[42] found a predictable correlation in the spectra of diverse carboxylic acid crystals, between the forbidden transition probability and the electronic structure of carboxylic acid molecules. If carboxyl groups are linked directly with aromatic rings, or with other large π-electronic systems, the forbidden transition is of ca. three times higher intensity than in the case when the same π-electronic systems are separated from carboxyl groups by methylene groups.[49] The effect of the symmetry breaking parameter η is illustrated in Figure 8.

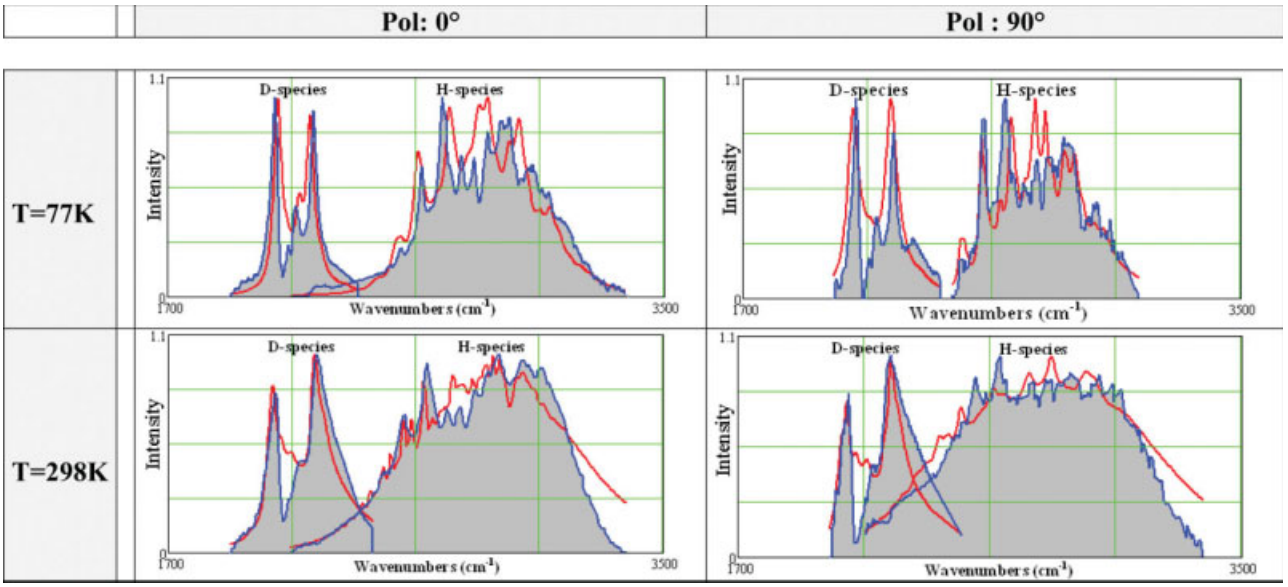

Figure 6. Effects of temperature and isotopic substitution on the spectral densities of crystalline 3-thiophenic acid at different polarizations and without Fermi resonances. Experiment: grayed spectra. Theoretical: thick red line. The corresponding parameters are given in Table 1.

This inability to reproduce some details of the fine structure was yet met for precedent works using the same model and dealing with other more complex molecules.[50–52] It may be explained by the fact that the model used ignored the anharmonicity of the fast modes[53] and the electrical anharmonicity which is a quite strong effect that cannot be discarded in the in the area of the infrared line shape of stretching mode υ_{X-H} of H-bonded species, especially for H-bonded system in polar solvents.[54]

Let us comment the magnitude of the indirect damping parameters. The values of the parameters used by us for crystalline 3TPA acid are of the same magnitude as those used previously by Blaise et al.,[12] in a study dealing with acetic acid in the gas phase, except for the indirect damping at 300 K which is 0.1Ω

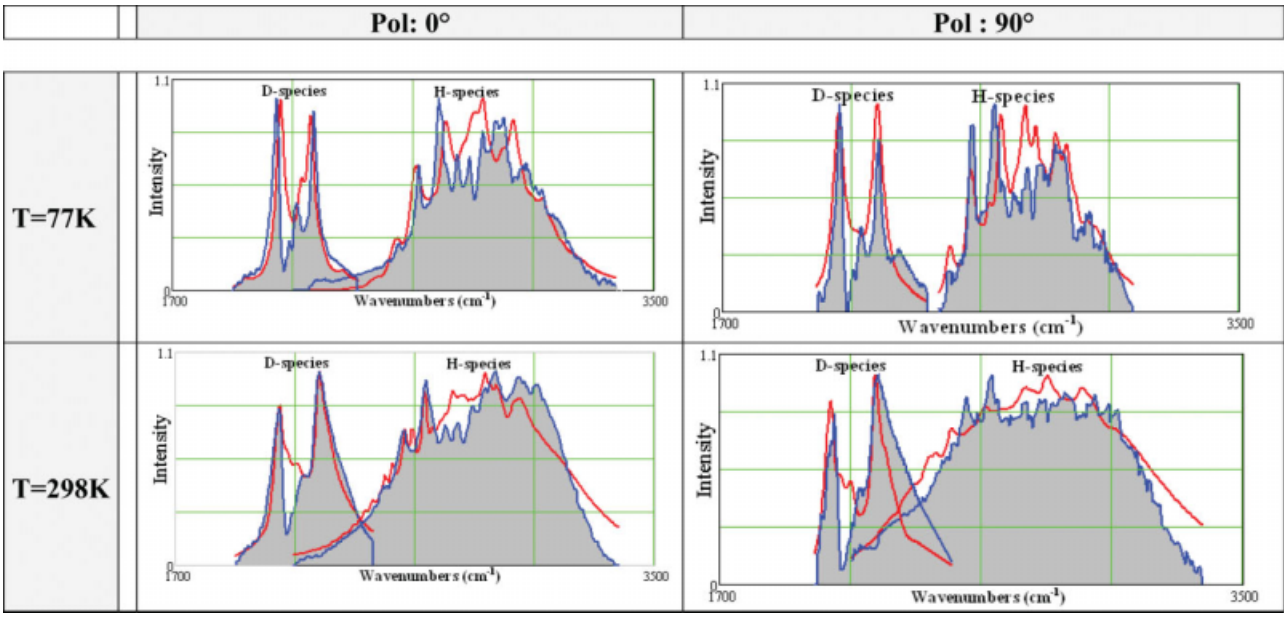

Figure 7. Effects of temperature and isotopic substitution on the spectral densities of crystalline 3-thiophenic acid at different polarizations and three Fermi resonances. Experiment: grayed spectra. Theoretical: thick red line. The corresponding parameters are given in Table 2.

Table 3. Fermi Parameters (in cm^{-1}) Used to Reproduce the Theoretical 3-Thiophenic-H Acid Line Shapes.

H-species Pol (°)	T (K)	Δ_1	Δ_2	Δ_3	f_1	f_2	f_3	γ_1^δ	γ_2^δ	γ_3^δ
0	77	−130	100	80	10	15	10	0.1	0.04	0.1
90	77	−140	150	−120	10	10	5	0.2	0.02	0.01
0	298	−550	−300	200	40	10	20	0.4	0.1	0.2
90	298	−180	130	120	10	20	10	0.2	0.1	0.02

for 3TPA acid, whereas it is equal 1Ω for acetic acid. One may ask whether the indirect damping used for crystalline state is weaker than that used for the gaseous phase because the indirect relaxation is ought to be larger in the solid state. The reason is that in the gas phase the indirect damping is an effective one which is the result of the combination of the indirect damping and of the rotational structure.[55] There have been some quantum attempts to introduce for weak H bonds the damping of the fast mode ("direct relaxation") or damping of the H-bond bridge vibration (indirect relaxation): Rösch and Ratner[18] have treated the relaxation of the fast mode, whereas Boulil et al.,[25] have considered that of the H-bond bridge. If direct damping leads to the whole broadening of the line shape via simple exponential decay factor[56] (each Dirac-delta peak of the quantum theory is transformed into Lorentzian of the same width), the indirect damping induces subtle modifications by changing in complex situations both frequencies and relative intensities which are accompanied by the whole narrowing.[56] The quantum theory of indirect damping takes a classical limit[27] when the H-bond bridge is assumed to be described by a stochastic classical variable. This classical limit model predicts, similar as the quantum one, a narrowing of the line shape. When it is assumed that the thermal averaging of a stochastic variable, and the integration over time of this variable commute, then the classical limit transforms into the semiclassical model of Yarwood and Robertson[28,29] which predicts a broadening in place of narrowing. At last, the Robertson and Yarwood model of indirect relaxation reduces, in the slow modulation limit to the pioneering Bratos model[30] of relaxation which initiated the series of works on the IR line shapes of weak H bonds within the linear response theory.[57] It seems therefore that the quantum theories of direct and indirect dampings, which are working within the strong anharmonic coupling theory and the linear response theory, are benchmarks in the challenge dealing with the IR features of H-bonded species.

In a recent important article, Luckhaus,[58] has studied the effect of conformational relaxation on the quantum dynamics of the hydrogen exchange tunneling in the D_{2h} subspace of formic acid dimer. The results which support the vibrational assignment of Madeja and Havenith.[59] Moreover, the fully coupled ro-vibrational calculations used by Luckhaus[58] demonstrate the compatibility of experimentally observed inertia defects with in-plane hydrogen exchange tunneling dynamics in formic acid dimer.

In other important article, dynamical dimensionality of the intramolecular proton transfer motion in formimidol, was examined theoretically at the QCISD(T) level by Spirko et al.[60] The examination consisted in constructing adiabatic surfaces of the bond lengths and angles of the skeletal atoms as functions of the proton transfer coordinates. The shapes of "geometry" surfaces have revealed many sizable couplings between the proton transfer and remaining vibrational motions making evident the necessity of their explicit accounting in reliable modeling. It is interest to note that in this pioneering study, greater quantitative insight was obtained by evaluating the vibrational energies of

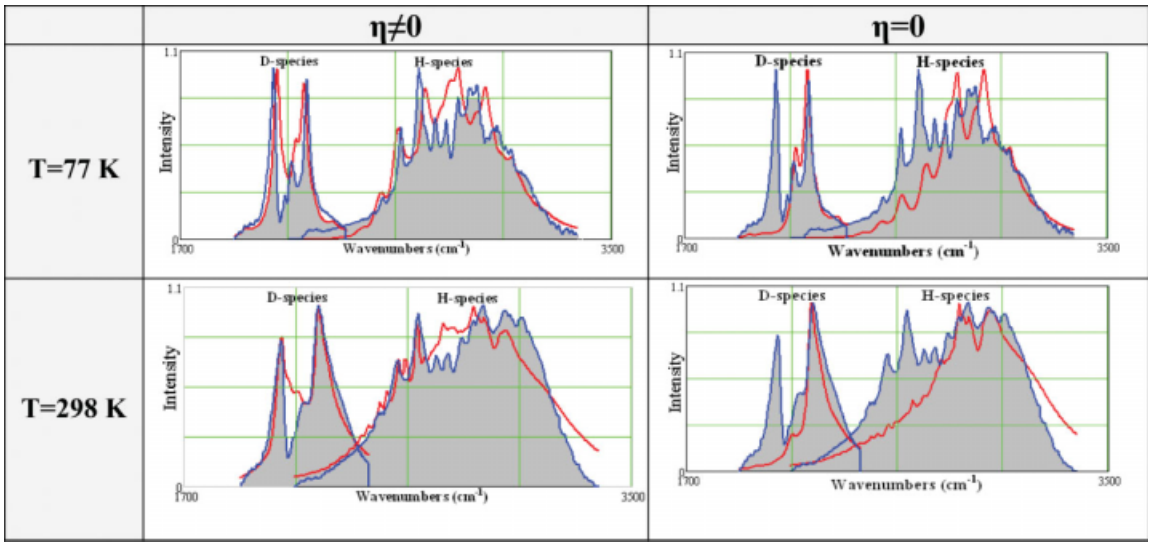

Figure 8. Comparison between theoretical and experimental line shapes of crystalline 3-thiophenic acid involving three Fermi resonances. Effect of the forbidden transition parameter η. Experimental: grayed spectra. Theoretical: thick red line. The values of the parameters involved in the computations are given in Tables 1 and 2.

Table 4. Fermi Parameters (in cm^{-1}) Used to Reproduce the Theoretical 3-Thiophenic-D Acid Line Shapes.

D-species Pol (°)	T (K)	Δ_1	Δ_2	Δ_3	f_1	f_2	f_3	γ_1^δ	γ_2^δ	γ_3^δ
0	77	180	−100	−180	20	10	20	0.02	0.1	0.01
90	77	−180	−250	−300	15	10	20	0.04	0.1	0.2
0	298	−550	−300	200	40	10	20	0.4	0.1	0.2
90	298	−180	−150	120	20	10	10	0.4	0.02	0.1

the hydrogen bonding modes (explicitly accounted) as functions of the skeletal modes (adiabatically accounted). Although the calculations are approximate, the approach of Spirko et al.[60] provide enough evidence for a very strong coupling between the intramolecular proton transfer motions and the skeletal bending motions.

It should be stressed that in our simulations we have assumed, following Maréchal and Witkowski,[19] only the first-order dependence of the angular frequency of the fast modes on the coordinate of the slow modes (Q_i) [see eq. (11)] and we have neglected the modulation of the equilibrium positions of the fast modes and the quadratic dependence of their frequencies on (Q_i)[38] as confirmed by several experimental correlations.[61,62] It is of interest to note that the use of quadratic modulation of the angular frequency $\omega(Q_i)$ of the fast modes and their equilibrium position q_e (Q_i) by the hydrogen bond distances (Q_i), which can be represented by two expansions to the second order: $\omega(\mathbf{Q}) = \omega^\circ + \alpha\mathbf{Q} + \beta\mathbf{Q}^2$ and $q_e(\mathbf{Q}) = q_e^\circ + f^\circ\mathbf{Q} + \mathbf{g}^\circ\mathbf{Q}^2$ must be taken into account in order to increase the level density and spectral features of 3-thiophenic and its deuterated derivative. At last, the magnitudes of the damping parameters and of the Davydov coupling parameter are near the same at 77 and 298 K. The same constation was elicited for the 3-thiophenic-D. The Davydov coupling parameters employed here are similar to those used by Maréchal and Witkowski.[19] We have also used for damping parameters, values near to those used by Blaise et al.[12]

Finally, this model reproduces less easily the corresponding line shapes of crystalline 3-thiophenic acid even after incorporation of Fermi resonances between some bending modes involving the vibrations of the C—H bonds of the aromatic rings, the O—D species being less satisfactorily reproduced than the corresponding O—H species.

Conclusion

In this work, we have proposed a general quantum theoretical approach of the υ_{X-H} infrared spectra of crystalline centrosymmetric cyclic dimers of H-bonded species. This approach, applied to crystalline 3-thiophenic acid, is dealing with the strong anharmonic coupling theory within the linear response theory and takes into account Davydov coupling, Fermi resonances, and direct and indirect quantum relaxations. The intrinsic anharmonicity of the slow mode has been introduced by use of Morse potential whereas the fast mode was assumed to harmonic. At last, it seems necessary to assume some degree of forbidden transition in order to obtain a good fitting between the evaluated spectra and the experimental ones.

Our approach reproduces satisfactorily the main features of the experimental line shapes of 3-thiophenic and its deuterated derivative for two different temperatures (77 and 298 K), especially for the high and low frequencies tails, but less satisfactorily the details of the fine structure. The inability to reproduce some details of the fine structure may be explained by the fact that the model used involving some important approximations especially neglect of the anharmonicity of the fast mode, electrical anharmonicity and quadratic dependence of the angular frequency of the fast mode and its equilibrium position on the H-bond bridge elongation. We leave for future the treatment of the general problem of hydrogen-bonds involving together all missed approximations with the ingredient of the present approach.

References

1. Pimentel, G.; McCellan, A. The Hydrogen Bond; Freeman: San Francisco, 1960.
2. Bratos, S.; Hadzi, J. J Chem Phys 1957, 27, 991.
3. Sandorfy, C. In Topics in Current Chemistry, Vol. 120; Springer: Berlin, 1984; p. 41.
4. Maréchal, Y. In Molecular Interaction; Orville-Thomas, W., Eds.; Wiley: New York, 1980; p. 230.
5. Maréchal, Y. In Vibrational Spectra and Structure; Vol. 16; Durig, J., Eds.; Elsevier: Amsterdam, 1987; p. 312.
6. Henri-Rousseau, O.; Blaise, P. In Theoretical Treatment of Hydrogen Bonding; Hadzi, D., Eds.; Wiley: New York, 1997; p. 165.
7. Louisell, W.; Walker, L. Phys Rev 1965, 137, 204.
8. Rekik, N.; Ghalla, H.; Oujia, B.; Michta, A.; Flakus, H. T. Chem Phys (Submitted).
9. Morse, P. M. Phys Rev 1929, 34, 57.
10. Kubo, R. J Phys Soc Jpn 1957, 12, 570.
11. Kubo, R. In Lectures in Theoretical Physics I; Brittin, W. E.; Dunham, L. G., Eds.; Interscience: Boulder, 1958; p. 151.
12. Blaise, P.; Wojcik, M. J.; Henri-Rousseau, O. J. Chem Phys 2005, 122, 64306.
13. Blaise, P.; El-Amine Benmalti, M.; Henri Rousseau, O. J Chem Phys 2006, 124, 024514.
14. Hudson, P.; Robertson, J. H. Acta Cryst 1964, 17, 1497.
15. Flakus, H. T. J Mol Struct 2003, 646, 15.
16. Flakus, H. T.; Pyzik, A. Chem Phys 2006, 323, 479.
17. Flakus, H. T.; Chelmecki, M. Spectrochim Acta A 2001, 58, 179.
18. Rösch, N.; Ratner, M. J Chem Phys 1974, 61, 3344.
19. Maréchal, Y.; Witkowski, A. J Chem Phys 1968, 48, 3637.
20. Rekik, N.; Velescu, A. J Mol Struct (THEOCHEM) 2003, 620, 265.
21. Chamma, D.; Henri-Rousseau, O. Chem Phys 1998, 229, 51.
22. Blaise, P.; Henri-Rousseau, O.; Grandjean, A. Chem Phys 1999, 244, 405.
23. Benmalti, M. E.-A.; Chamma, D.; Blaise, P.; Henri-Rousseau, O. J Mol Struct 2006, 785, 27.
24. Benmalti, M. E.-A.; Blaise, P.; Flakus, H. T.; Henri-Rousseau, O. Chem Phys 2006, 320, 267.
25. Boulil, B.; Henri-Rousseau, O.; Blaise, P. Chem Phys 1988, 126, 263.
26. Boulil, B.; Déjardin, J.-L.; El-Ghandour, N.; Henri-Rousseau, O. J Mol Struct (THEOCHEM) 1994, 31, 83.
27. Blaise, P.; Déjardin, P.-M.; Henri-Rousseau, O. Chem Phys 2005, 313, 177.

28. Yarwood, J.; Robertson, G. Nature 1975, 257, 41.
29. Robertson, G.; Yarwood, J. Chem Phys 1978, 32, 267.
30. Bratos, S. J Chem Phys 1975, 63, 3499.
31. Bratos, S.; Ratajczak, H. J Chem Phys 1982, 77, 76.
32. Flakus, H. T. Chem Phys 1981, 62, 103.
33. Wojcik, M. J. Int J Quantum Chem 1976, 10, 747.
34. Rekik, N.; Issaoui, N.; Ghalla, H.; Oujia, B.; Wójcik, M. J. J Mol Struct (THEOCHEM) 2007, 9, 821.
35. Belhayara, K.; Chamma, D.; Henri-Rousseau, O. J Mol Struct 2003, 648, 93.
36. Witkowski, A.; Wojcik, M. Chem Phys 1973, 1, 9.
37. Odinokov, S. E.; Iogansen, A. V. Spectrochim Acta 1972, 28A, 2343.
38. Rekik, N.; Ghalla, H.; Issaoui, N.; Oujia, B.; Wójcik, M. J. J Mol Struct (THEOCHEM) 2007, 821, 58.
39. Boczar, M.; Wójcik, M. J.; Szczeponek, K.; Jamróz, D.; Zieba, A.; Kawalek, B. Chem Phys 2003, 286, 63.
40. Leviel, J. L.; Maréchal, Y. J Chem Phys 1971, 54, 1104.
41. Wojcik, M. J. Int J Quantum Chem 1986, 29, 855.
42. Flakus, H. T. J Mol Struct (THEOCHEM) 1989, 187, 35.
43. Flakus, H. T.; Miros, A. J Mol Struct 1999, 484, 103.
44. Flakus, H. T.; Miros, A. Spectrochim Acta 2001, A57, 2391.
45. Flakus, H. T.; Chelmecki, M. Spectrochim Acta Part A 2002, 58, 179.
46. Flakus, H. T.; Chelmecki, M. J Mol Struct 2004, 705, 81.
47. Flakus, H. T.; Jablonska, M. J Mol Struct 2004, 707, 97.
48. Flakus, H. T.; Miros, A.; Jones, P. G. J Mol Struct 2002, 604, 29.
49. Flakus, H. T.; Jablonska, M.; Jones, P. G. Spectrochim Acta Part A 2006, 481, 65.
50. Boczar, M.; Wojcik, M. J.; Szczeponek, K.; Jamroz, D.; Zieba, A.; Kawalek, B. Chem Phys 2003, 286, 63.
51. Wojcik, M. J. Chem Phys Lett 1981, 503, 83.
52. Boczar, M.; Szczeponek, K.; Wojcik, M. J.; Paluszkiewicz, C. J Mol Struct 2004, 700, 39.
53. Rekik, N.; Velescu, A.; Blaise, P.; Henri-Rousseau, O. Chem Phys 2001, 273, 11.
54. Yukhnevich, G. V.; Tarakanova, E. G. J Mol Struct 1998, 447, 257.
55. Belhayara, Kh.; Chamma, D.; Velcescu, A.; Henri-Rousseau, O. J Mol Struct 2007, 65, 833.
56. Henri-Rousseau, O.; Blaise, P.; Chamma, D. In Infrared Line Shapes of Weak Hydrogen Bonds: Recent Quantum Developments, Vol. 121: Advances in Chemical Physics; Prigogine, I.; Rice, S. A., Eds.; Wiley: New York, 2002; p. 241.
57. (a) Bratos, S.; Leicknam, J.-Cl. J Chem Phys 1994, 101, 4536; (b) Bratos, S.; Leicknam, J.-Cl. J Chem Phys 1995, 103, 4887.
58. Luckhaus, D. J Phys Chem A 2006, 110, 3151.
59. Madeja, F.; Havenith, M. J Chem Phys 2002, 117, 7162.
60. Spirko, V.; Cejchan, A.; Lutchyn, R.; Leszczynski, J. Chem Phys Lett 2002, 355, 319.
61. Novak, A. Struct Bonding 1974, 18, 177.
62. Olovsson, I.; Jönsson, P.-G. In Hydrogen Bond; Scheuster, P.; Zundel, G.; Sandorfy, C., Eds.; North Holland: Amsterdam, 1976.